Arbitrarily shaped Dual–stacked Patch Antennas: A Hybrid FEM Simulation

Jian Gong and John L. Volakis
Radiation Laboratory
Department of Electrical Engin. and Comp. Sci.
University of Michigan
Ann Arbor, MI 48109-2212

Abstract

A dual–stacked patch antenna is analyzed using a hybrid finite element - boundary integral (FE-BI) method. The metallic patches of the antenna are modeled as perfectly electric conducting (PEC) plates stacked on top of two different dielectric layers. The antenna patches may be of any shape and the lower patch is fed by a coaxial cable from underneath the ground plane or by an aperture coupled microstrip line. The ability of the hybrid FEM technique for the stacked patch antenna characterization will be stressed, and the EM coupling mechanism is also discussed with the aid of the computed near field patterns around the patches.

I. Introduction

Since being proposed, the dual stacked patch antennas received tremendous attention mainly because of the drastic improvement of their operational bandwidth in comparison to the inherent narrow band feature of single patch configurations. Further bandwidth improvement was also reported by employing an aperture coupled microstrip line, where the lower patch is electromagnetically coupled to a microstrip line through an opening at the ground

plane. This design was shown capable of achieving over 10% bandwidth. Certain numerical approaches for extensive analysis of non-rectangular single patch antennas with an aperture coupled feed have been investigated (e.g. [1, 2]). Unfortunately reports for non-rectangular stacked structure analyses have not been seen in the literature, except for experimental results published in [3, 4]). An analysis was only reported in [5] where the Hankel transform was employed on the assumption that the feed structure is absent from the analytical system. This implies that any change in the resonance due to the feed can not be modeled using this technique. A comprehensive simulation for stacked non-rectangular patch configurations is therefore desired for design purposes. This is the motivation of this report and we will discuss both probe and aperture coupled feeds. The former offers flexibility in the feeding network layout and makes the feed design separable from that of antenna elements [3], whereas the latter design, while challenging for most of the existing methodologies, is readily incorporated into our proposed hybrid FEM formulation, especially when the patches and the coupling opening (aperture) are non-rectangular for wider bandwidth designs.

In the following sections, we first briefly describe the hybrid FEM formulation as applied to the patch antenna analysis. More detailed discussions of the numerical approach may be found in [6] and [7]. Using our numerical simulator for characterizing the antenna's dielectric and geometric parameters, we concentrate on the microstrip feed line modeling with the aid of an FEM connectivity scheme. Some results for a circular stacked-patch antenna will be presented to show the ability of the technique, and typical computed 3-D near field distributions around the patches inside the two dielectric layers are displayed for visualization which reveals the insight of the EM coupling mechanism between the two patches.

II. Hybrid FEM Formulation

Consider the configuration of a stacked circular patch antenna shown in Figure 1, where a cavity encompassing the patches is recessed in the ground plane to simulate the truncation of the computational region V. As described in [6], the finite element method (FEM) is employed to model the fields in the three dimensional volume, whereas a boundary integral equation on the aperture of the cavity (excluding the metallic patch area) is built up based upon the equivalence principle to associate the radiated fields in the region above

the ground plane to those in the cavity so that the continuity conditions of the tangential fields across the aperture is inherently imposed. (Interested Readers are referred to [6] for detailed discussions and mathematical derivations.) It should be noted that the edge-based tetrahedral elements were used for the 3-D cavity fields and the triangular surface elements for the aperture fields simulation. The reasons are twofold (a) the edge elements have shown a precise representation of the vectorial electromagnetic fields without spurious modes; (b). arbitrarily shaped geometries and more sophisticated feeding schemes (e.g. aperture coupled stripline, microstrip line, equi-potential model for coaxial cable [8], etc.) are easier to model using edge elements. After the standard discretization and assembly procedures, we obtain a system of equations in a matrix form as

$$\sum_{j}^{N_V} [A_{i^v j}] \left\{ E_j^v \right\} + \sum_{j}^{N_S} [B_{i^v j}] \left\{ E_j^s \right\} = \{ K_{i^v} \}, \quad i = 1, 2, ..., N^V \tag{1}$$

where i^v and i^s represent the unknown indices in the cavity and on the aperture, respectively, and the former contains the latter in global numbering since the aperture fields E_j^s are part of the cavity fields E_j^v. N_V and N_S are the number of cavity and aperture edges that do not lie on any PEC surfaces. It is apparent that the total number of the system unknowns is N_V and, in most cases, $N_S \ll N_V$. This property is important because $[A_{i^v j}]$ is a sparse system although $[B_{i^v j}]$ is a full matrix. Thus the storage requirement is insignificant for this exact boundary truncation, which governs the modeling accuracy for the radiation problems.

In the case of stacked patch antennas, the lower patch is usually placed close to the cavity's base, which is treated as a grounded PEC wall. Hence, inside the FEM cavity, the lower patch should also be modeled as a PEC plate. Two separate dielectric layers above and below this patch must be considered to account for the substrate effects. Indeed, an attractive feature of the FEM over integral equation method is its capability to model multilayer structures with the same case as it does with the homogeneous structures.

III. Feed Simulations

Probe Feed

For the radiation analysis of a probe-fed patch antenna, we use the infinitesimally thin current source which is chosen to coincide with some mesh element edge. In this fashion, the excitation term $\{K_{iv}\}$ is usually modeled such that all the entries are set to zero except for those coincident with the probe(s) which link the patch and the ground plane. Specifically, if the probes are assumed to have a constant current $I_i, i = 1, 2, M_p$ (M_p is the number of the probes), then the excitation entries associated with the corresponding edges may be written as

$$K_i = -jkZ_0 I_i l_i, \tag{2}$$

where k is the free space wave number, Z_0 is the free space intrinsic wave impedance and l_i is the length of the i^{th} edge. The phase difference between different probes may be readily represented by the phasor notation of each complex current I_i. Once the system of equations are solved, the input impedance is found to be

$$Z_{in} = \frac{E_i l_i}{I_i}, \tag{3}$$

where E_i denotes the calculated field along the i^{th} edge of length l_i. The radiation pattern may be obtained by integrating the computed aperture fields with the far–zone approximation of the dyadic Green's function in the presence of an infinitely large PEC ground plane.

Microstrip line Feed

When the stacked patch antenna is fed with a microstrip line network underneath the ground plane (cavity's base) via a coupling aperture (see Figure 2), special treatment for the feed structure must be considered in the FEM formulation. This is because the microstrip line is usually designed to have different size and shape as compared to the cavity's geometric parameters. In addition, the microstrip line used as a transmission line, in most cases, carries traveling waves, thus, changing the field behavior in the cavity. Hence, the conventional FEM simulation treating the entire 3-D domain in a same fashion is not appropriate for this problem.

Consider the structure to be modeled as shown in Figure 3. In this case, it is appropriate to separate the computational domains because of the small element size required in modeling the feed structure. One difficulty encountered when this decomposition is implemented is how one must model the coupling through the aperture. (We consider in this report a rectangular aperture which has been extensively employed in practice. Other aperture shapes for wideband consideration have also been seen in the literature and this formulation can be readily extended for those designs.) As described in [6], the cavity fields are discretized using tetrahedral elements, whereas in the microstrip line rectangular brick elements are considered the best candidates for field modeling. The selection of brick elements is particularly useful because of the geometry and the field property of the microstrip line, and it is shown that this choice retains better accuracy and efficiency in comparison to other element selections. As shown in Figure 4, although both types of elements employ edge–based field expansions, the meshes across the common area (coupling aperture) are different, and this causes the inconsistency for the field representation in the formulation. In the implementation, this implies that the usual boundary condition for the tangential field continuity across the aperture can not be enforced in a straightforward manner.

We observe that the aperture is narrow in shape along the microstrip line and this fact allows us to assume a 'static' field feature for a given frequency. Therefore, the 'potential' concept may be applied to the problem in order to relate the fields below and above the aperture. Specifically, we enforce the 'equi–potential' continuity condition, which states that: the potential across the narrow aperture due to the field distribution in the cavity region must be equal to that due to the microstrip line excitation. If the edges are classified as

in mesh (b):

- $E_j^{b1} \quad j = 1, 2, 3, \ldots$ *vertical edges*
- $E_j^{b2} \quad j = 1, 2, 3, \ldots$ *diagonal edges*

in mesh (c):

- $E_j^{c} \quad j = 1, 2, 3, \ldots$ *vertical edgesonly*

then the 'equi–potential' continuity condition is expressed as

$$E_j^{b1} = \epsilon_j E_j^{c} \tag{4}$$

$$E_j^{b2} = \frac{t}{2d}(\epsilon_j E_j^c + \epsilon_{j+1} E_{j+1}^c), \tag{5}$$

where

$$\epsilon_j = \begin{cases} 1 \\ -1 \end{cases}, \tag{6}$$

t and d are the lengths of vertical and diagonal edges, respectively. (Thus, t happens to be the width of the narrow rectangular aperture.)

The connectivity scheme for entirely different computational domains may be extended by generalizing this concept. It is apparent that this approach makes the FEM implementation straightforward for different geometry/size domains that would be significantly inefficient if only one type of elements were used for modeling the structure. In addition, this technique ensures the system condition since the number of distorted elements in the mesh are minimized.

Results

As an example, a circular stacked patch antenna was used as shown in Figure 1, where the geometry parameters were designed for the antenna to be operated in the frequency range from 7 to 9 GHz. When excited using a microstrip line, it is observed that the field across the coupling aperture has a Gaussian–like distribution, as expected. Figure 5 shows the gain computed as a function of frequency and as seen, the design is indeed wideband, as promised. Figure 6–9 show the radiation patterns for both polarizations in the E–plane and H–plane, respectively, and Figure 10 plots the input impedance, whose VSWR is 2:1, corresponding to a bandwidth of 15%. In Figure 11, we show the magnitude of the computed field distribution on the antenna's radiating aperture when a probe feed was employed for excitation. It is noted that the energy is concentrated on the two opposite sides of the top patch and that the PEC cavity wall has little effect on the field near the antenna edges. Also, we observe from Figure 12 that the field couples to the lower patch from two locations even though only one probe is used for excitation.

References

[1] D. Zheng and K.A. Michalski, "Analysis of coaxial fed antennas of arbitrary shape with thick substrates," *J. Electromagn. Waves Appl.*, Vol. 25, No. 12, pp. 1303–1327, 1991

[2] J. Zheng and D.C. Chang, "End-Correction Network of a Coaxial Probe for Microstrip Paths Antennas,' *IEEE Trans. Antennas Propagat.*, Vol. 39, No.1, January 1991

[3] C.H. Chen, A. Tulintseff and R.M. Sorbello, *IEEE AP-S/URSI Symposium Digest*, pp 251–254, 1984

[4] Albert Sabban, "A New Broadband Stacked Two–layer Microstrip Antenna," *IEEE AP-S/URSI Symposium Digest*, pp. 63–66, 1983.

[5] K. Araki, H. Ueda and T. Masayuki, "Numerical Analysis of Circular Disk Microstrip Antenna With Parasitic Elements," *IEEE Trans. Antennas Propagat.*, Vol. 34, No. 12, pp 1390–1394, December, 1986

[6] J. Gong, J.L. Volakis, A.C. Woo and H. T. G. Wang, "A Hybrid Finite Element-Boundary Integral Method for the Analysis of Cavity-backed Antennas of Arbitrary Shape," *IEEE Trans Antenna and Propagat.*, Vol. 42, No. 9, pp 1233–1242, September 1994

[7] J.L. Volakis, J. Gong and A. Alexanian, "Electromagnetic Scattering From Microstrip Patch Antennas and Spirals Residing in a Cavity," *Electromagnetics*, Vol. 14, No. 1, pp 63–85, 1994

[8] J. Gong and J.L. Volakis, "An Efficient and Accurate Model For Coax Cable Feeding Structure Using Finite Element Method," Submitted to *IEEE Trans Antenna and Propagat.* for publication, 1994

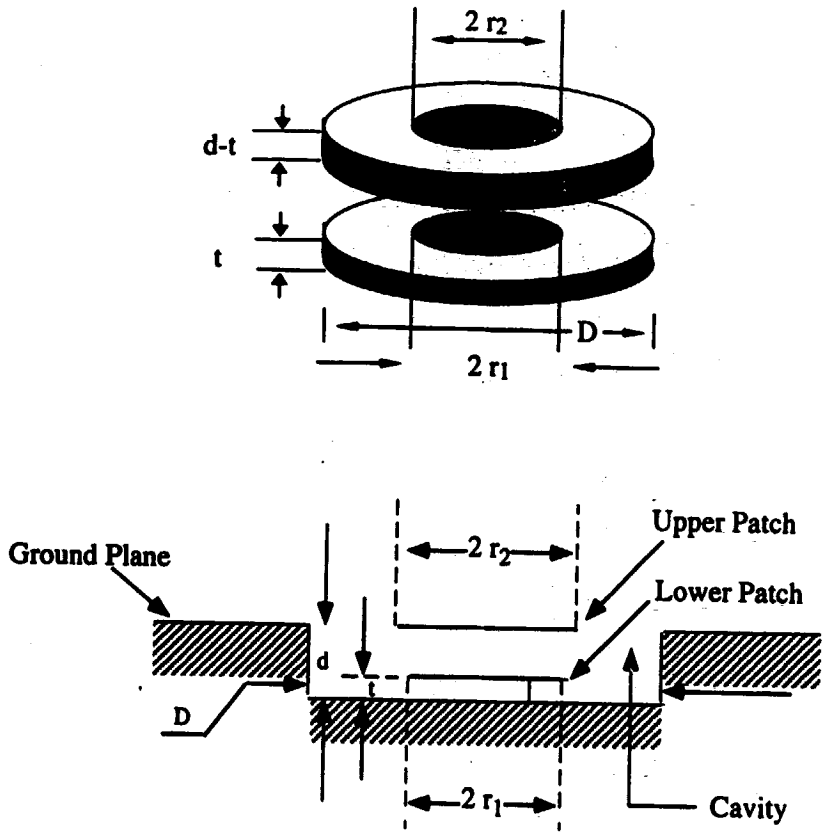

Figure 1: Illustration of A Cavity-backed Stacked Circular Patch Antenna, which could be fed by a probe or by an aperture coupled microstrip line.

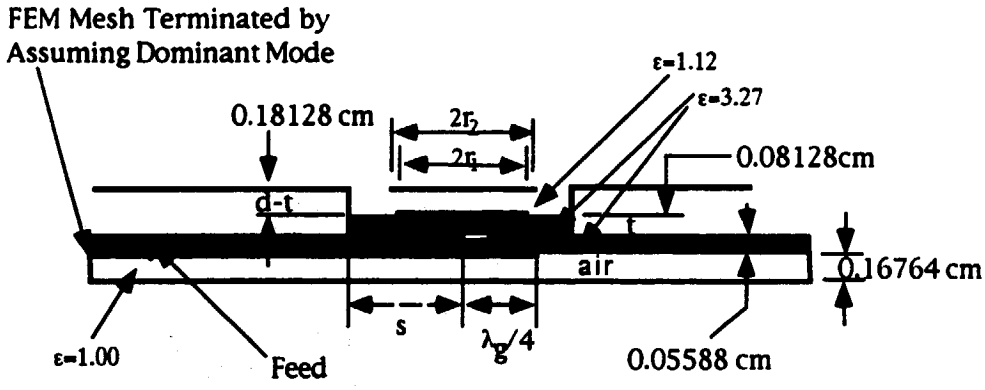

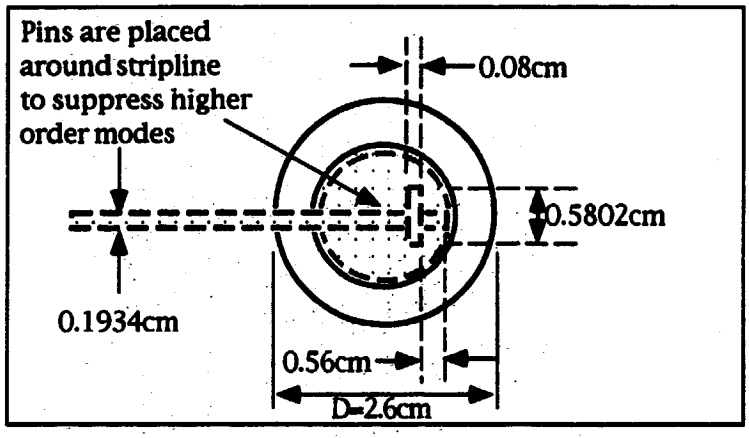

r_1 = 0.65 cm
r_2 = 0.75cm
t = 0.08128 cm
d-t = 0.18128 cm
d= 0.26256 cm
s=0.2145cm

slot width=0.04 cm
λ_g= guided wavelength

D = 2.6 cm* * Calculations were done using this cavity size. Thus, performance will remain unchanged when array elements are separated by comparable distances. Tighter placement requires further investigation to maintain performance within specs.

Figure 2: A stacked circular patch antenna with a microstrip line feed. The design of geometric and dielectric parameters will be used for modeling.

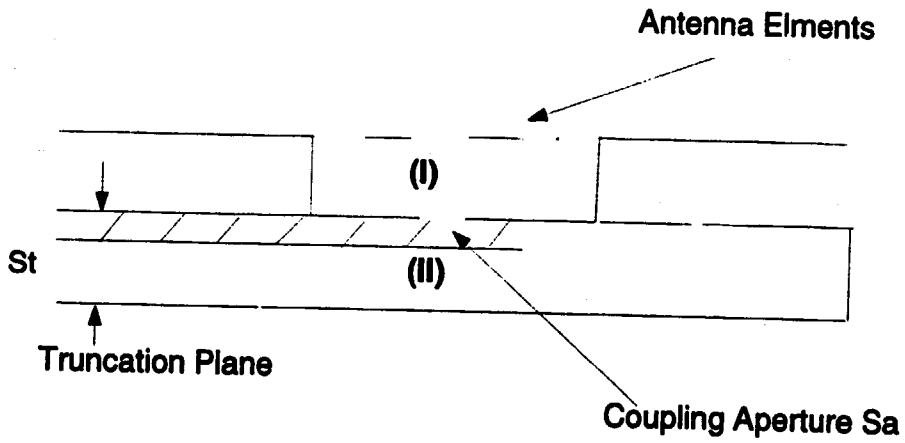

Figure 3: Cross–section of an aperture coupled patch antenna, showing the cavity region I and the microstrip line region II for two different FEM computation domains.

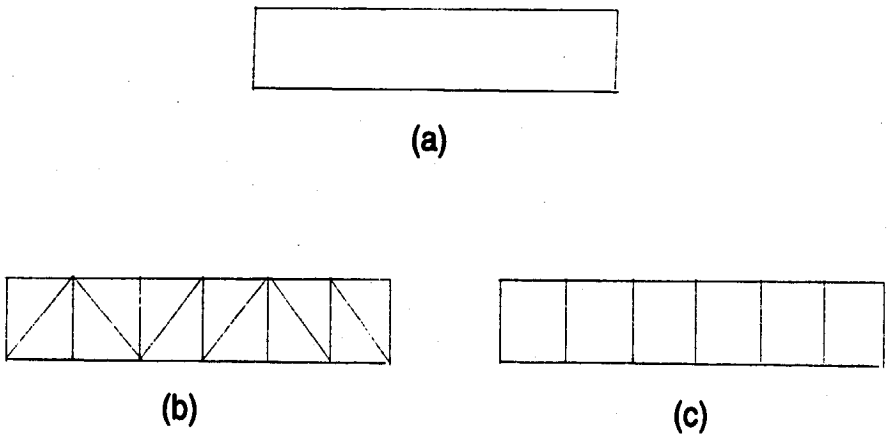

Figure 4: (a). a rectangular aperture; (b). a typical mesh from cavity region I ; (c). the uniform mesh from microstrip line region II.

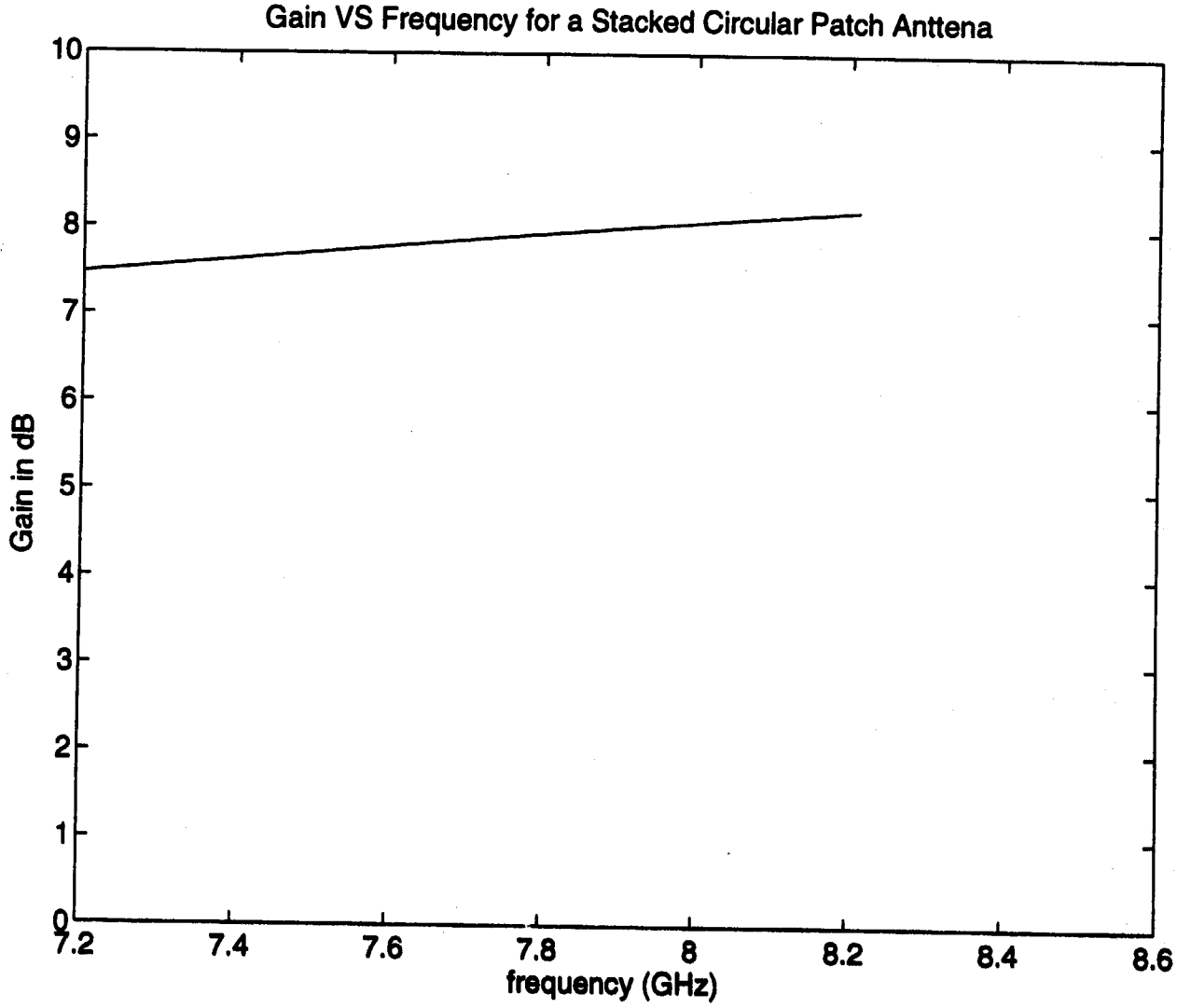

Figure 5: The gain pattern vs. freqency in GHz for circular stacked patch antenna.

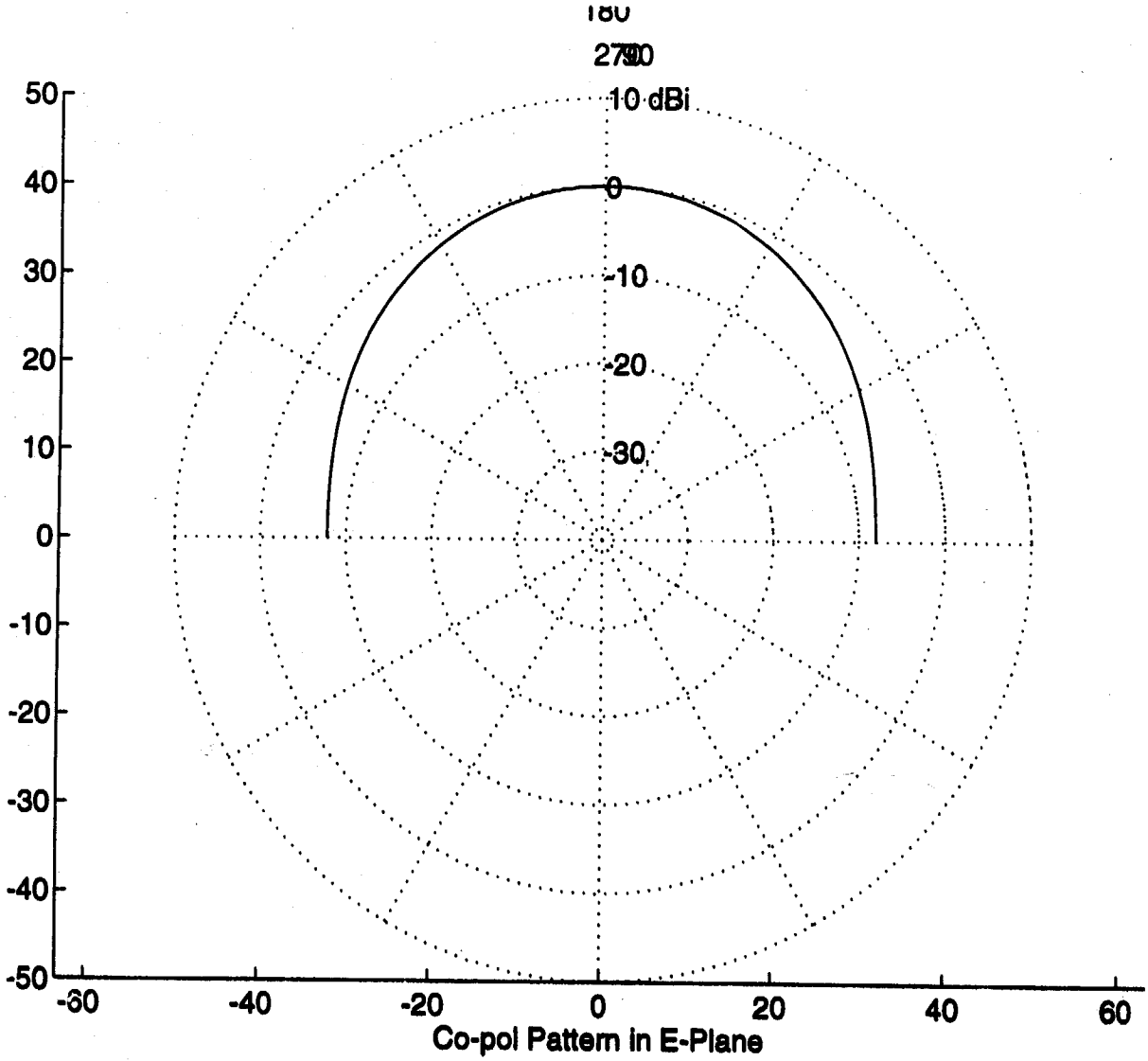
180
270
90
10 dBi
0
-10
-20
-30
50
40
30
20
10
0
-10
-20
-30
-40
-50
-60
-40
-20
0
20
40
60
Co-pol Pattern in E-Plane

Figure 6:

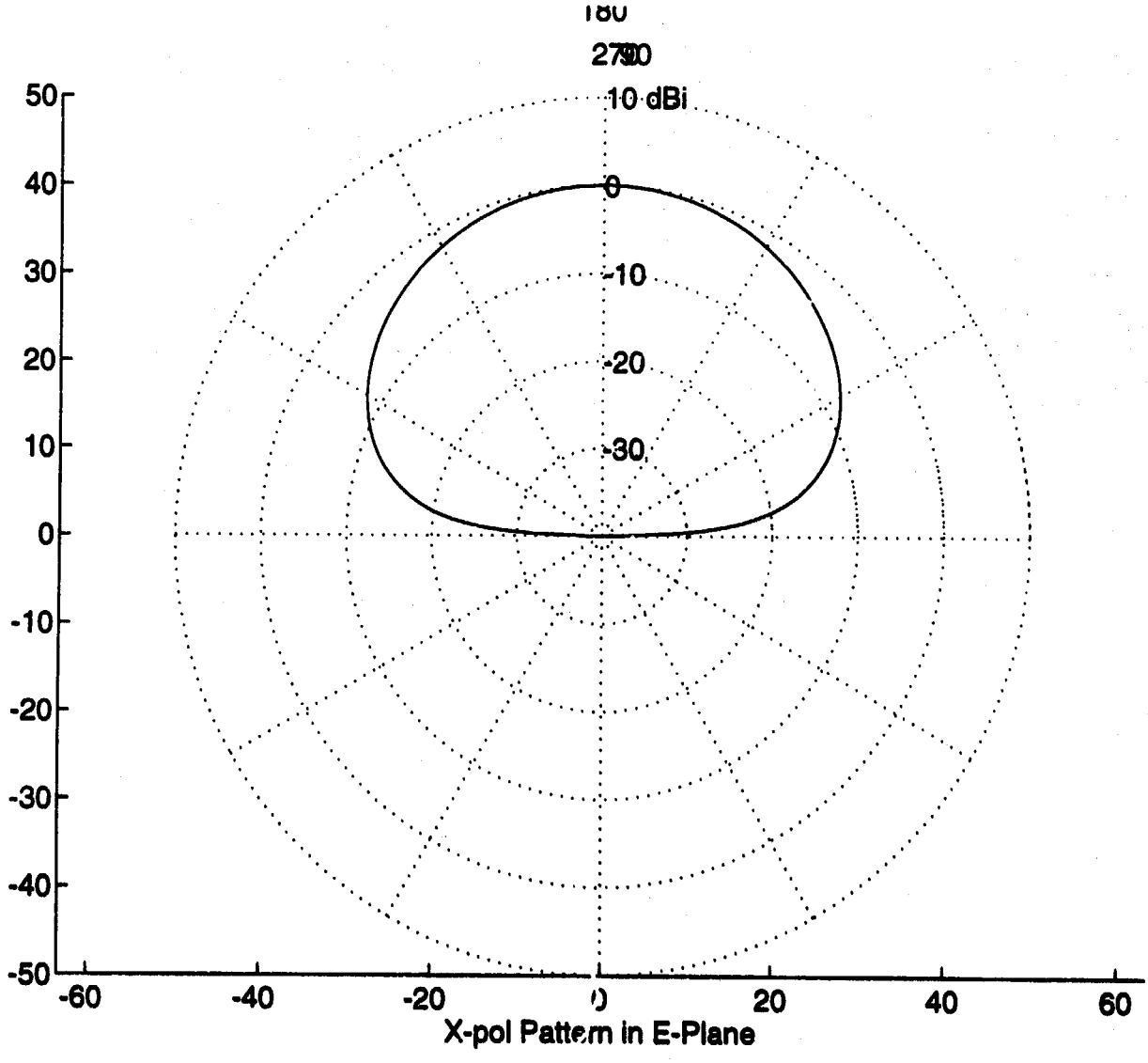
180
270
90
10 dBi
0
-10
-20
-30
50
40
30
20
10
0
-10
-20
-30
-40
-50
-60
-40
-20
0
20
40
60
X-pol Pattern in E-Plane

Figure 7:

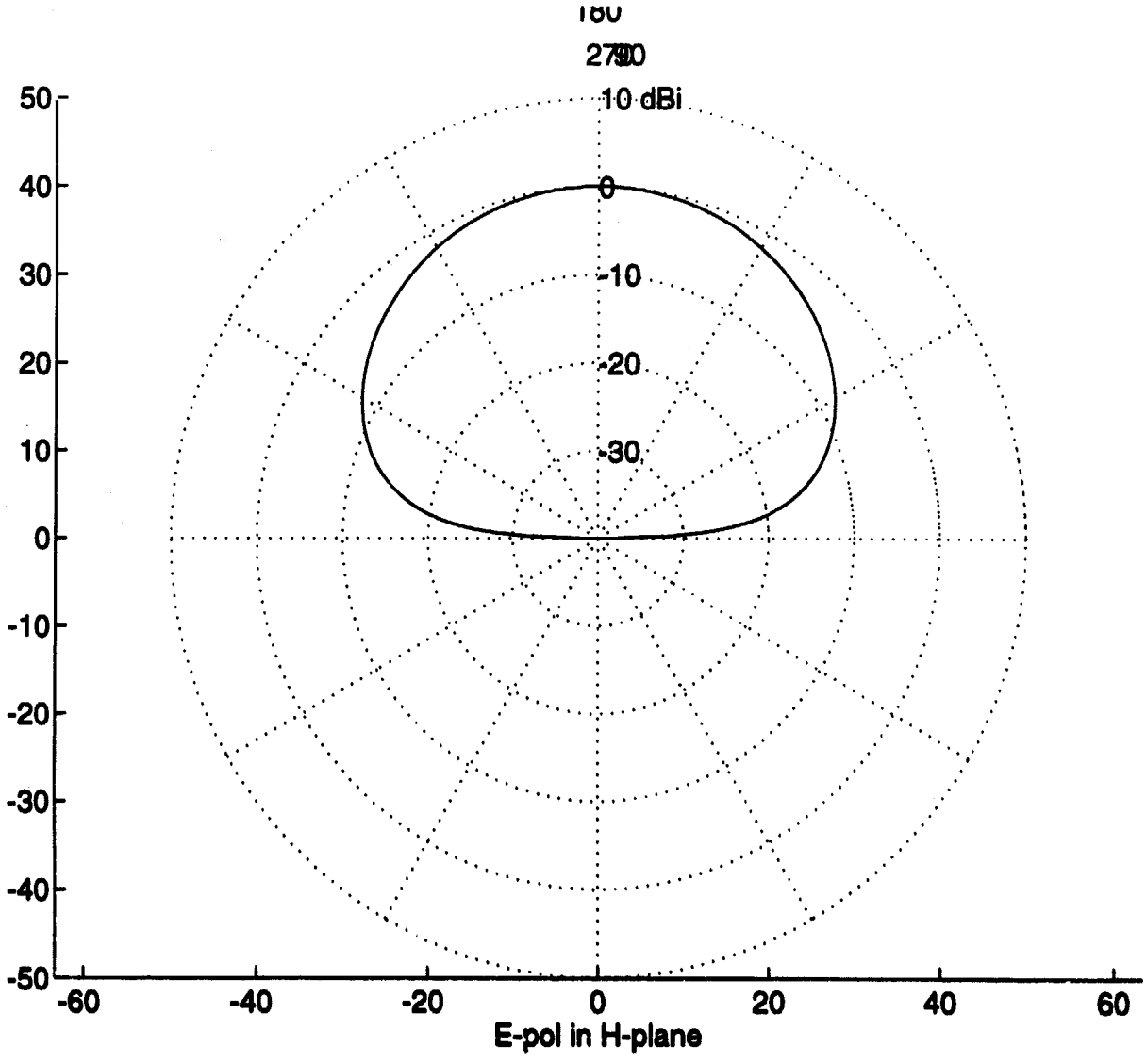
180
270
90
10 dBi
0
-10
-20
-30
50
40
30
20
10
0
-10
-20
-30
-40
-50
-60
-40
-20
0
20
40
60
E-pol in H-plane

Figure 8:

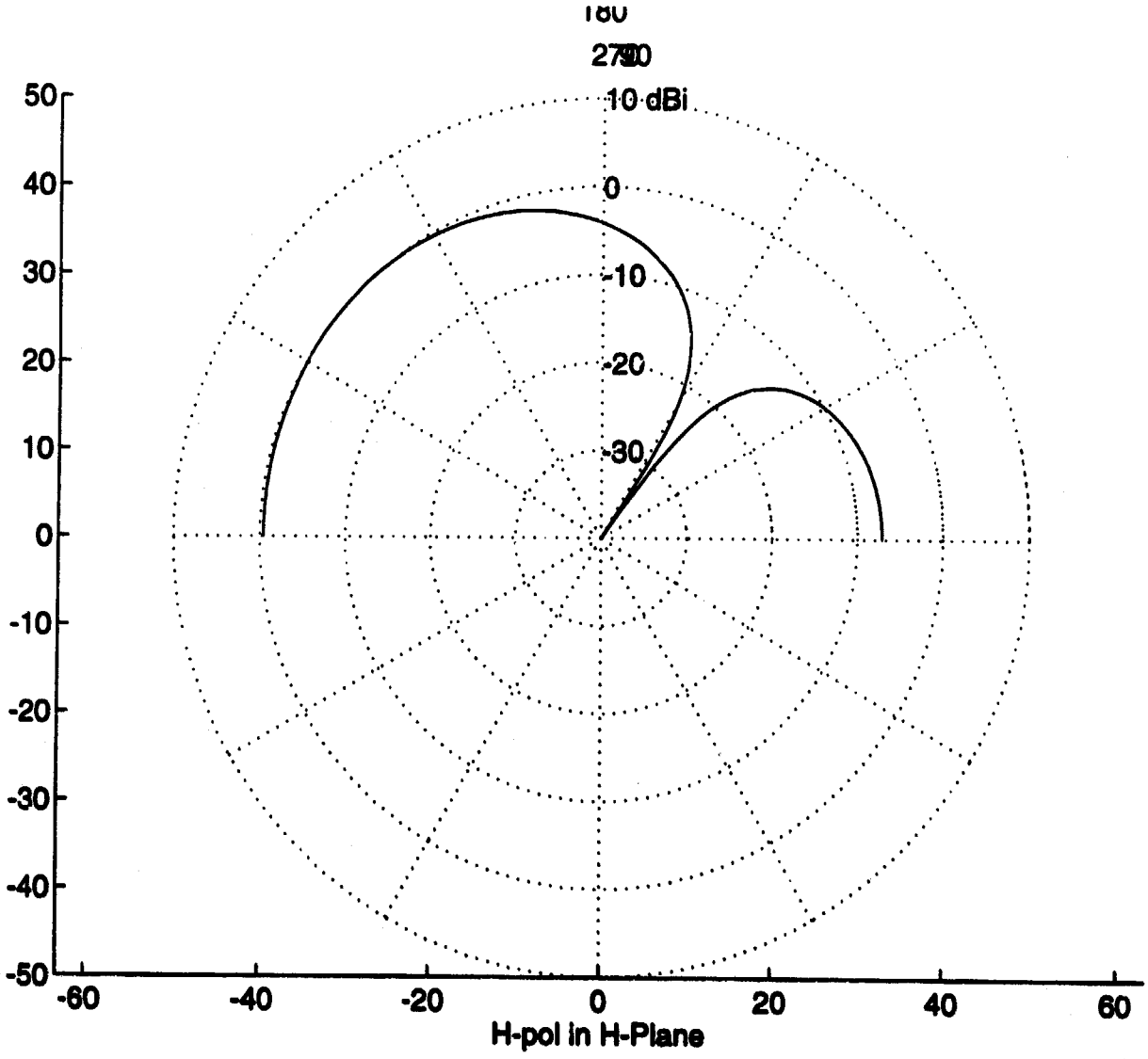
180
270
10 dBi
0
-10
-20
-30
50
40
30
20
10
0
-10
-20
-30
-40
-50
-60
-40
-20
0
20
40
60
H-pol in H-Plane

Figure 9:

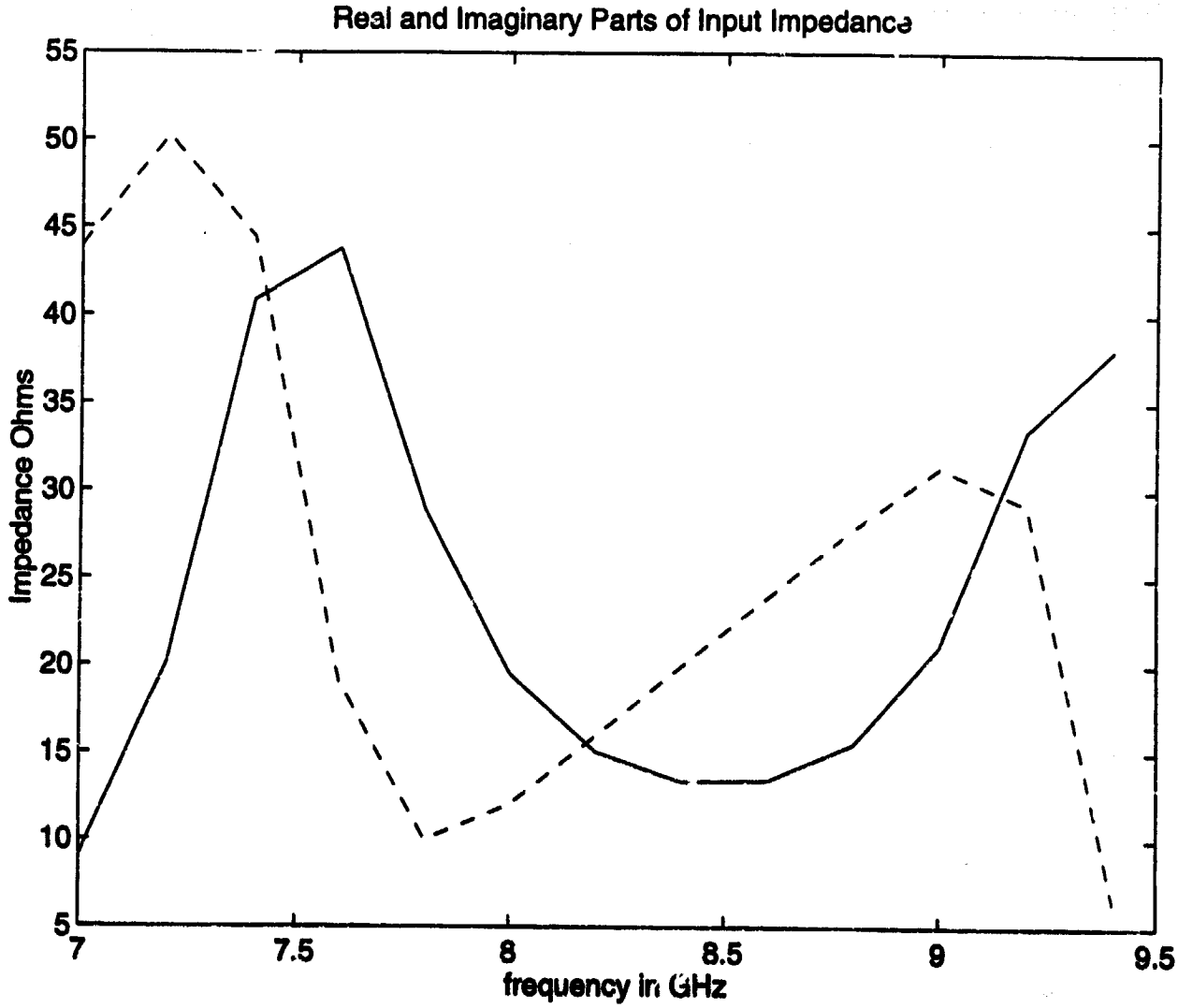

Figure 10: Input impedance vs. frequency in GHz for the circular stacked patch antenna. Solid line is for real part and dashed line for imaginary part.

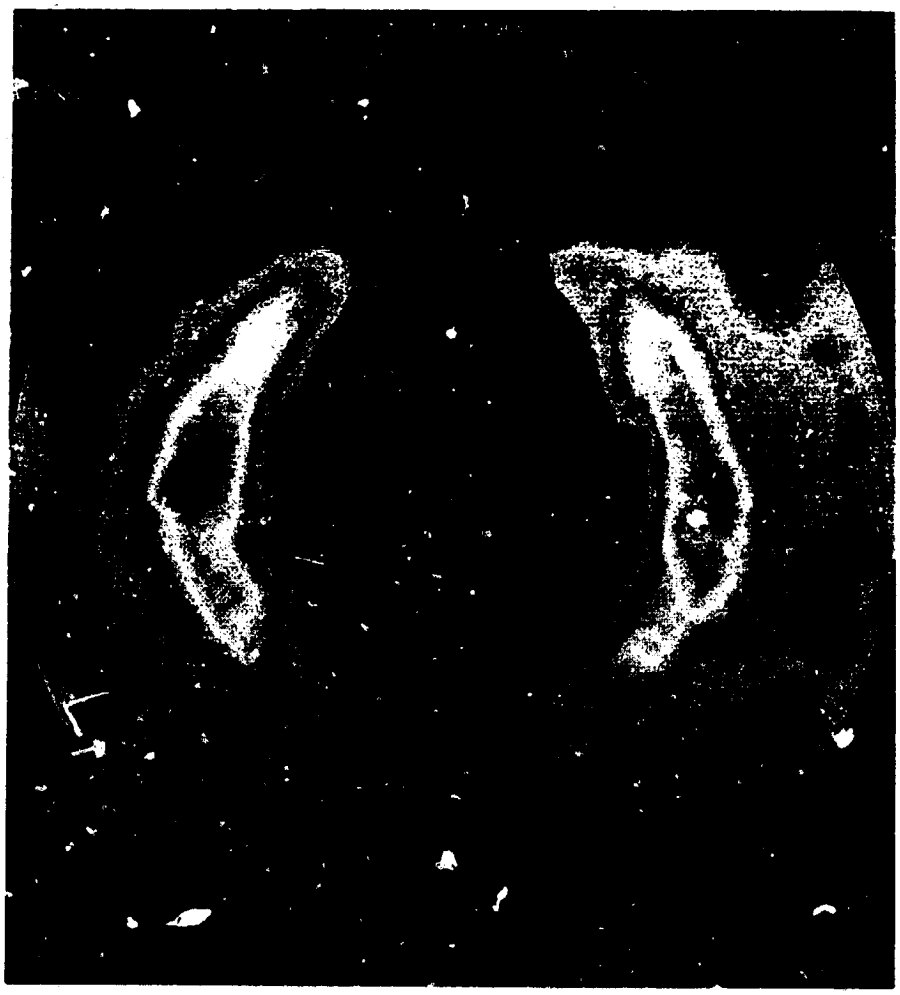

Figure 11: The field magnitude distribution on the antenna's radiating aperture. It is shown that the energy is concentrated on two opposite sides of the top patch and that the PEC cavity wall has little effect on the field.

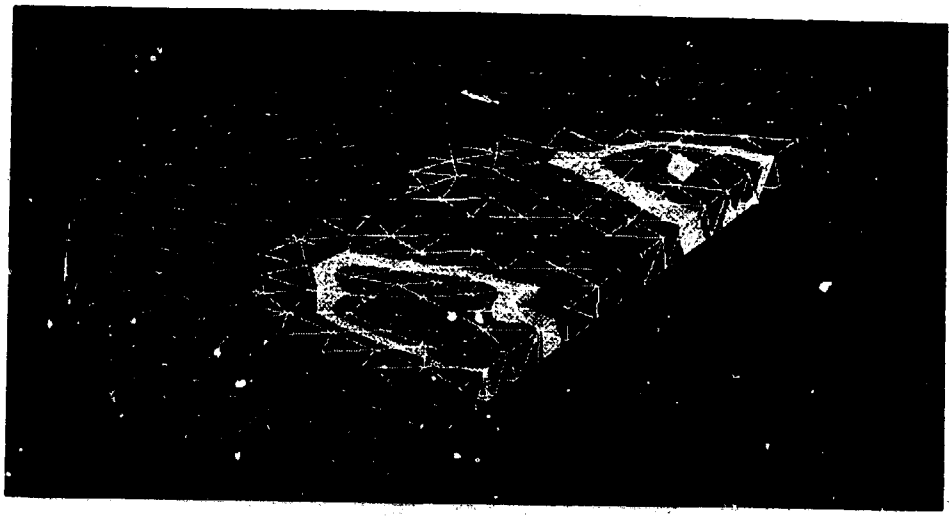

Figure 12: The field magnitude distribution within the cavity of the antenna excited by a probe. It is shown that the energy couples to the lower patch from two locations even though only one probe is utilized for excitation.